DETERMINISTIC ANALYSIS OF EXTREME ROLL MOTIONS USING TAILORED WAVE SEQUENCES

Günther F. Clauss, Technical University Berlin (Germany)
Janou Hennig, Technical University Berlin (Germany)

Abstract

Encountering a freak wave remains one of the most horrible visions for a ship master. Until now the mechanisms which underlie large rolling and subsequent capsizing due to a rogue wave are only partly disclosed.

In the framework of the German research project ROLL-S which is funded by the German Federal Ministry of Research and Education (BMBF) nine partners are cooperating on the investigation of large rolling and capsizing mechanisms covering fields like numerical analysis and simulation, validation, and evaluation of capsizing risk.

The project part presented here deals with the validation of numerical tools for the analysis of large rolling and capsizing. The main goal is the implementation of a sophisticated capsizing test procedure. For providing useful data for the analysis of the capsizing process as well as for the validation of numerical methods, exact correlation of wave excitation and ship rolling is indispensable.

All wave trains are tailored for the specific purpose of each capsizing test and generated in the model tank. Unusual wave trains like regular waves followed by a freak wave and special wave groups within a defined random sea as well as realistic wave scenarios have been generated.

The parameters of the model seas are systematically varied to investigate the ship model response with regard to metacentric height, model velocity, and course angle for different ship types. The wave elevation at the position of the ship model in time and space is calculated (and controlled by registrations during model tests) in order to relate wave excitation to the resulting roll motion.

Figure 1: Rogue wave estimated at 60 feet moving toward ship in the Gulf Stream off Charleston, South Carolina, with light winds of 15 knots (picture taken fromhttp : //www.mpc.ncep.noaa.gov/).

1. INTRODUCTION

Encountering a freak wave such as shown in Fig. 1 remains one of the most horrible visions for a ship master. Until now the mechanisms which underlie large rolling and subsequent capsizing due to a rogue wave are only partly disclosed. Within the last decade, more than hundred large tankers and container ships have been lost in severe weather conditions, some of them due to the interaction with giant waves or dangerous wave groups causing large rolls angles [8], [11]. Recent incidents like the particular average of the German cruise liner Bremen [16] illustrate the fatal risk of freak waves and document the importance of detailed knowledge of the processes leading to large roll angles and capsizing. Therefore numerous research projects deal with the hydrodynamic analysis of wave/ structure interaction and the wave itself.

In the framework of the German research project ROLL-S which is funded by the German Federal Ministry of Research and Education (BMBF) nine partners are cooperating on the investigation of large rolling and capsizing mechanisms covering fields like numerical analysis and simulation, validation, and evaluation of capsizing risk: Flensburg Shipyard (FSG), Gerhard Mercator University in Duisburg, German Lloyd, Hamburg Ship Model Basin (HSVA), MTG Marinetechnik GmbH, Seacos, Technical University Berlin (TUB), and Technical University Hamburg-Harburg.

The project part presented here deals with the validation of numerical tools for the analysis of large rolling and capsizing. The main goal is the implementation of a sophisticated capsizing test procedure. Presently the following aims have been achieved:

• Fully automated motion measurement of a free running ship model at HSVA [14]

• Improvement of wave generation techniques:

  – Adaptation and implementation for the linear wave generation technique at HSVA

  – Further development and application of the non-linear technique for the generation of high transient wave packets at HSVA.

  – Non-linear transformation of design wave sequences from stationary wave probes to the moving ship model (moving reference frame)

  – Generation of complex deterministic wave scenarios for capsizing tests

• Evaluation of capsizing test results

2. CONCEPT OF COMPUTER CONTROLLED CAPSIZING TESTS

Analyzing the process of large rolling and capsizing has to consider the following wave characteristics:

- extreme wave height and wave steepness
- wave groupiness
- propagation velocity and direction

Unfavorable phase relations of wave components as well as detrimental wave/ structure interactions lead to dangerous situations such as

- loss of stability at the wave crest
- resonant excitation, esp. parametric rolling
- broaching due to a loss of course stability.

Analysis of these complex, non-linear mechanisms puts high demands on the capsizing test set up and procedure:

- exact correlation of cause (wave excitation) and reaction (ship motion)
- reproducibility, high accuracy at measurement and control units
- deterministic course of test events.

These demands have been realized by a sophisticated test procedure at HSVA [14]. Fig. 2 shows the principle test configuration for computer controlled sea-keeping tests.

Three main system components are coordinated:

- wave maker
- towing carriage (including the horizontal carriage)
- ship model.

In head seas, the ship is positioned at the side wall of the tank's end, opposite to the wave maker position. In seas from astern, the ship model has to wait close to the wave maker until a defined sequence of the wave train has passed.

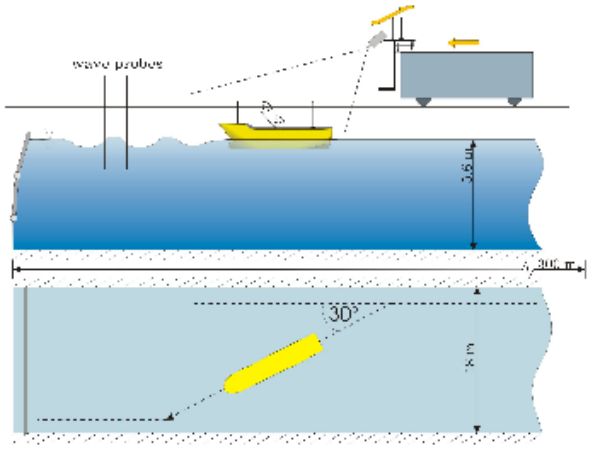

Figure 2: Configuration for computer controlled sea-keeping tests at HSVA.

As illustrated in Fig. 3 the test procedure starts with the definition of test parameters such as wave frequency ω (either as single frequency or an entire band/range), a characteristic wave height (e. g. the maximum wave crest elevation ζ_{max}) and the target position of the ship encountering the tailored wave train, x_e, related to the position of the maximum wave elevation x_c. These parameters are feeded into both the wave generation program and the test simulation program. As a first step the control signals for the flaps of the wave maker are calculated, i. e. flap angles as time series. Preprocessing includes the calculation of the encounter point in time and space where the ship meets the wave train under defined conditions. The software tool "WaveShipSim" returns the time t_e at which the ship will reach the encounter position x_e (depending on the target ship velocity υ_{mod} and course μ).

The two-paddle wave maker generates the specified wave train which has been selected for an individual test. The model starts to sail through the tank in such a way that it reaches the encounter position at the required time step. For keeping the given parameters constant, the propulsion is controlled over the entire run.

The ship moves in parallel with the tank side wall at a required minimum distance. Registration starts by setting the desired course.

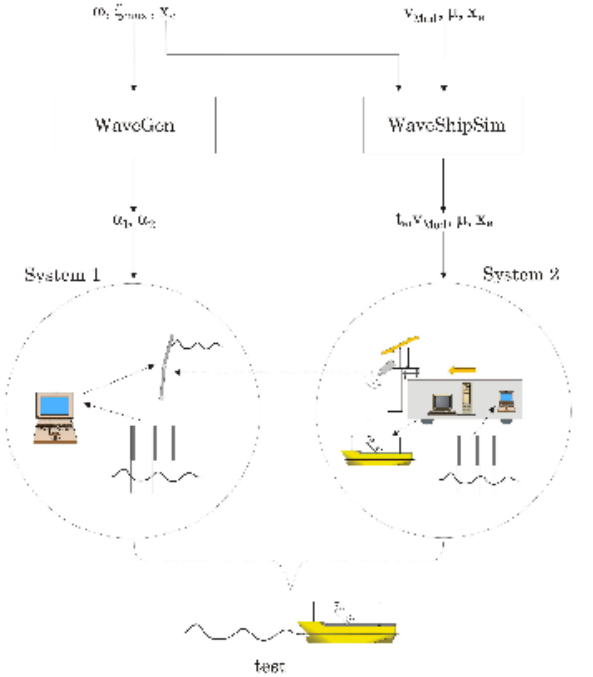

Figure 3: Computer controlled capsizing test procedure.

The ship's course is controlled by the master computer by telemetry which commands a Z-manoeuvre at constant course angle and model velocity. These test parameters as well as the model sea parameters are varied according to the metacentric height, GM, of the model, the expected rolling mode and occurrence of resonance. Ship motions in six degrees of freedom are registered precisely by computer controlled guidance of both, the towing and the horizontal carriage: During the entire test run, the ship model stays in the field of vision of the optical system line cameras. Additionally, the wave train is measured at several fixed positions of the wave tank.

When the model reaches the critical safety limit at the wave maker or the absorbers at the opposite side of the tank, the ship and the carriage stops automatically.

Thus, the test is realized by a deterministic course of test events which allows a reproducible correlation of wave excitation and ship motion.

3. GENERATION OF TAILORED WAVE SEQUENCES AND THEIR CORRELATION TO SHIP MOTIONS

There is a wide range of outstanding methods for the design and computer simulation of rogue wave events. However, the wave analysis techniques presented here serve as a practical method for generating waves tailored specifically for capsizing tests.

3.1. Wave generation

The wave generation process is illustrated in Fig. 4 for a two flap wave maker.

1. The target position in time and space is selected - for example the position where the ship encounters the wave train at a given time. At this location, the target wave train is designed – either with chosen parameters or an existing wave registration measured in a storm.
2. This wave train is transformed upstream to the position of the wave maker.
3. The corresponding control signals are calculated using adequate transfer functions of the wave generator.
4. This control signal is used to generate the specified wave train which is measured at the selected position in the tank. The ship model should arrive at the target position by the corresponding target time (measured from the beginning of the wave generation).
5. By registrations at the target position the compliance with the target wave parameters are validated.

On the basis of linear wave theory the specified amplitude distribution of the target wave train is given as Fourier spectrum $|\ddot{F}(\omega_j, x_c)|$.

Combined with the related phase spectrum at the concentration point x_c, $\varphi(\omega_j, x_c)$, we obtain the un-scaled Fourier transform at x_c:

$$\tilde{F}(\omega_j, x_c) = |\tilde{F}(\omega_j, x_c)|e^{i\varphi(\omega_j, x_c)}; \varphi = \omega_j t_i - k_j x_c \quad (1)$$

with circular frequency $\omega_j = j\Delta\omega$ as a function of wave number k_j , $t_i = i\Delta t$. The wave train is scaled due to the desired maximum wave elevation resulting in the Fourier transform $F(\omega_j, x_c)$ at x_c. Adaptation of the phase spectrum to the target location x_l gives the Fourier transform in x_l:

$$F(\omega_j, x_l) = |F(\omega_j, x_c)|e^{i(\omega_j t_i - k_j(x_c - x_l))}. \quad (2)$$

For reducing the number of time steps until the wave maker starts to operate, the wave train is shifted by time t_{shift}:

$$\hat{F}(\omega_j, x_0) = F(\omega_j, x_0) \cdot e^{-i\omega_j t_{shift}}. \quad (3)$$

Finally, this Fourier transform is multiplied by the hydrodynamic RAO (relating main board motion to wave elevation), the geometrical RAO, and the hydraulic RAO for each wave paddle. The geometric RAO assigns the paddle motion for a single flap to both flaps:

$$\alpha_{OK} = \tau\alpha_{vir}, \quad (4)$$
$$\alpha_{GK} = (1 - |\tau|)\alpha_{vir}. \quad (5)$$

$$\tau(\lambda) = 1, \quad \lambda < \lambda_0 \quad (6)$$
$$\tau(\lambda) = 1.5e^{-0.055(\lambda - \lambda_0)^2} - 0.5, \lambda \geq \lambda_0 \quad (7)$$

with $\lambda_0 = 2$ m.

3.2. Transient wave packets and tailored wave sequences

A ”transient wave packet” is defined as a special wave group consisting of subsequent waves with increasing propagation speeds so that all ”components” meet in the so-called concentration point before they diverge in opposite order (Fig. 5). Transient waves for model excitation have originally been proposed by [7] and further developed by [17], [1], and [2]. Transient wave packets are characterized by well-defined periods and phase relations, and are therefore predestined for capsizing tests because they

- have a short extension and consequently a small sensitivity with regard to disturbing frequencies, course deviation etc.
- are tailored for the test purpose with given geometric parameters like steep-ness at the encounter area of ship and wave
- allow the modelling of very high and steep wave combinations (freak or giant waves, see [12])
- can be generated as defined extreme events in a seaway (consideration of environment and history) or as solitary wave groups meeting the ship in parametric roll resonance motions (caused by regular waves).

Even extreme wave events can be modelled in the wave tank as shown in Fig. 6, which presents the simulation of the New Year Wave (which has been registered on January 1, 1995 by a down looking radar at the Draupner platform in the Norwegian Ekofisk field, [18], [9], [10]). Fig. 6 compares model test results (scale 1:81) at our tank of the Technical University Berlin (80 m long, 4m wide, water depth 1.5 m) with the New Year Wave registration. The measured wave train shows quite a good agreement with the target wave. This example demonstrates that the method is also adequate for the realization of high natural storm wave scenarios.

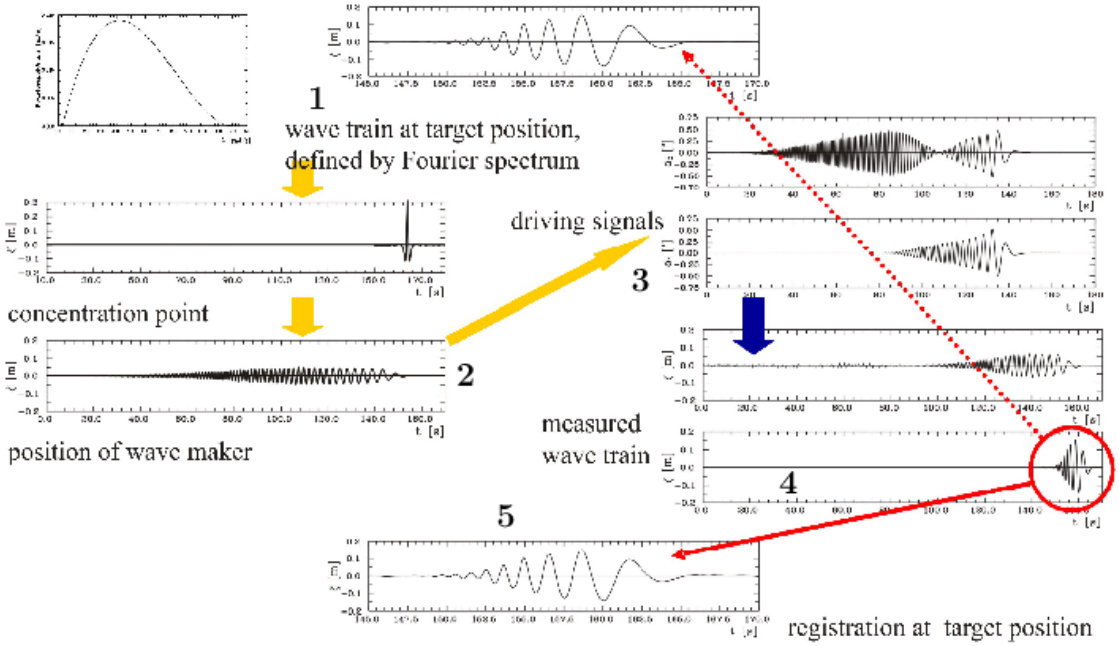

Figure 4: Principle of the wave generation process. Calculation starts from the desired target wave train.

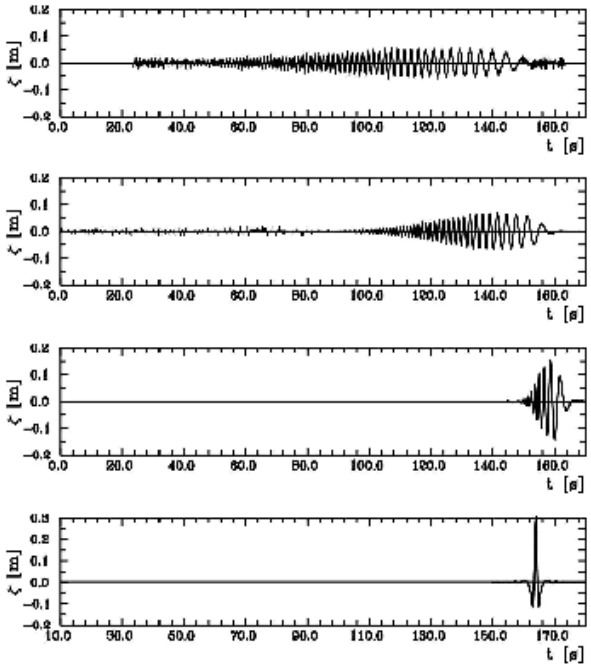

Figure 5: Generation of a transient wave packet: registrations at x =5.88 m, 47.74 m, and 85.16 m, concentration point at x =95.00 m (concentration point).

3.3. Correlation of wave excitation and ship motion

For providing useful data for the analysis of the capsizing process as well as for the validation of numerical methods, exact correlation of wave excitation and ship rolling is indispensable. This correlation is achieved by

- technical synchronization within an accurate test procedure, and
- knowledge of wave propagation.

For converting measured surface elevations linearly to arbitrary points in time and space, three cases are considered:

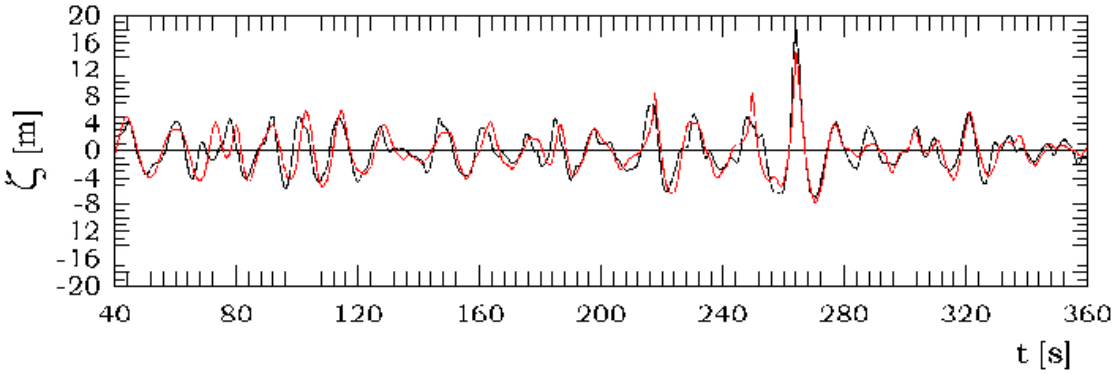

Figure 6: Draupner New Year Wave: Full scale data and wave tank generation (scale 1:81).

1. Let the registration of a wave train $\zeta(t_i, x_l)$ be given at the wave tank location x_l. The wave train at another fixed location x_{l+k}, $k \in Z_0$, is calculated by shifting the Fourier transform's phase by $k(x_{l+k} - x_l)$:

$$\zeta(t_i, x_{l+k}) = \frac{1}{2\pi} \sum_j F(\omega_j, x_l) \quad (8)$$

$$\cdot \; e^{i(\omega_j t_i - k(x_{l+k} - x_l))} \triangle\omega \quad (9)$$

2. Let the registration be taken under constant velocity υ_M = const. and encounter angle φ against the wave train. Thus the real wave numbers can be calculated from the encounter frequencies ω_{ej} by solving

$$\omega_j = \omega_{ej} + k(\omega_j) \cdot v_M \cdot \cos\varphi \quad (10)$$

numerically. Then, the above procedure is repeated.

3. For capsizing tests the undisturbed surface elevation at a ship's reference point is required. As this wave elevation cannot be measured directly it is calculated from a registration at another (fixed or constantly moving) location using the following scheme:

$$\omega_j = \omega_{ej} + k(\omega_j) \quad (11)$$

$$\cdot \; v_M(t_i) \cdot \cos\varphi(t_i)$$

$$\zeta(t_i, x_{l+k}(t_i)) = \frac{1}{2\pi} \sum_j F(\omega_j, x_l)$$

$$\cdot \; e^{i(\omega_j t_i - k_j \triangle x_i)} \triangle\omega \quad (12)$$

where Δx_i stands for the time varying distance between both locations.

Considering well-defined time windows during the test and excluding disturbances within the main signal, the described linear techniques can be applied to all types of model seas as well.

For steep wave trains - e. g. ratio of wave height to wave length is higher than 0.05 – the wave propagates faster than the corresponding linear wave. Furthermore, these waves show a crest-trough asymmetry increasing with wave height, and a mass transport in propagation direction. To synthesize steeper waves (up to freak waves) Kühnlein [13] proposed a method expanding the linear wave theory by evaluating the equations of orbital motions at the particles' real position and introducing an empirical term, which considers shallow water effects. This approach is complemented by introducing a wave packet description based on Stokes-III wave theory [15].

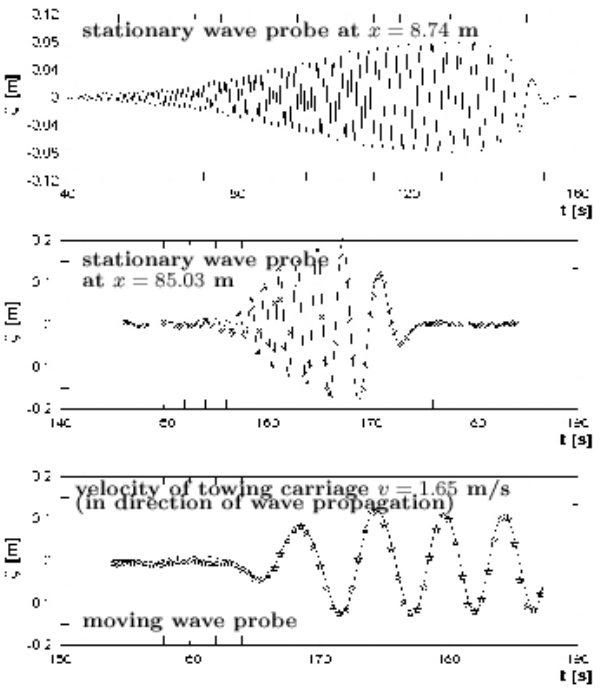

Figure 7: Registration of a wave packet at stationary wave probes and at a moving probe -comparison of calculation and registration

For a regular wave with circular frequency ω, amplitude ζ_a in water depth d the velocity potential and the surface elevation according to linear wave theory are given by

$$\phi(t,x,z) = \frac{\zeta_a g}{k}\frac{\cosh[k(z+d)]}{\sinh(kd)}\sin(\theta), \quad (13)$$

$$\zeta(t,x) = \zeta_a \cos(\theta), \quad (14)$$

$$\theta = kx - \omega t$$

g is the acceleration due to gravity, t denotes time, and (x, z) are space coordinates.

The particle velocities follow from the velocity potential:

$$u = \frac{\partial \phi}{\partial x}, \quad w = \frac{\partial \phi}{\partial z}. \quad (15)$$

From these velocities the particle elevations are derived using the Lagrangian frame [6].

For the domain Ω at time t = 0 and $(x_0, z_0) \in \Omega$ starting position of each particle, the positions at $t \geq 0$ are:

$$t = 0 : (x,z) = (x_0, z_0), \quad (16)$$

$$t > 0 : (x,z) = (x_0 + \alpha(t; x_0, z_0) + \gamma(t; x_0, z_0)) \quad (17)$$

with α and γ as particle elevations from rest in horizontal and vertical direction. Then

$$\frac{d\alpha}{dt} = \frac{\zeta_a \omega \cosh[k(z_0+\gamma+d)]}{\sinh(kd)}\cos(k(x_0+\alpha)-\omega t), \quad (18)$$

$$\frac{d\gamma}{dt} = \frac{\zeta_a \omega \sinh[k(z_0+\gamma+d)]}{\sinh(kd)}\sin(k(x_0+\alpha)-\omega t). \quad (19)$$

The expansion of the linear wave terms in (18) and (19) at the real position of the respective particle results in the surface elevation of a higher wave. The corresponding trajectories are not closed.

Since a higher wave propagates faster than a smaller one the dispersion relation has to be redefined. The wave number k follows from the ratio of circular frequency and wave celerity:

$$k = \frac{\omega}{c}. \quad (20)$$

The resulting phase velocity c is the sum of wave celerity $c_0 = \omega/k_0$ of a harmonic wave with frequency ω (according to linear theory) and a convective velocity at water surface u_z=0. This convection follows from the mass transport in the direction of wave propagation. Note that in the (closed) wave tank system a reverse flow is observed in addition to compensate for the convection mass flow [3], i. e.

$$c = c_0 + \overline{u}_{z=0} - \overline{u}_{ges}. \qquad (21)$$

The added velocity u_z=0 at the surface (averaged over time) follows from

$$\overline{u}_{z=0} = \int_0^{t_{end}} \frac{\alpha(\tau, x_0, z_0)}{t_{end}} d\tau. \qquad (22)$$

Similarly, we obtain the reverse current:

$$\overline{u}_{ges} = \int_0^{t_{end}} \int_{-d}^{0} \frac{\alpha(\tau, x_0, z_0)}{t_{end}} dz_0 d\tau. \qquad (23)$$

Solution of equations (18) to (23) gives the phase velocity c and the particle trajectories $\alpha(t; x_0, z_0)$ and $\gamma(t; x_0, z_0)$ of a high regular deep water wave with wave number k at each time step t.

From the particle trajectories (Lagrangian description) the surface elevation at $\alpha = x$ (Eulerian description) is calculated by iteration of:

$$\begin{aligned} \zeta(t,x) &= \{\gamma(\tau; x_0, z_0)|\tau = t; (x_0, z_0) \qquad (24) \\ &\quad (x = \alpha(\tau; x_0, z_0), z = 0)\}. \end{aligned}$$

Hence, the description of non-linear waves follows from the calculation of particle tracks using the Lagrangian frame. As a result, surface elevation is asymmetric, with steep crests and flat troughs. In addition, the particle paths are no longer closed as the orbital motion is superimposed on the convective flow in the direction of wave propagation.

Similar results follow from the Laplace equation if non-linear surface boundary conditions are introduced. If wave elevation and velocity potential are expanded as power series, with wave steepness $k\zeta_a$ being a small perturbation parameter, we obtain the Stokes higher order solutions. In case of a 3rd order Stokes wave the surface elevation results in

$$\begin{aligned} \zeta(t) = \frac{1}{k}(k\zeta_a)\cos\theta &+ \frac{1}{2}(k\zeta_a)^2\cos 2\theta \qquad (25) \\ &+ \frac{3}{8}(k\zeta_a)^3\cos 3\theta). \end{aligned}$$

The linear first term – the Airy wave – is modulated by small higher order terms which steepen the crest and induce a convective flow.

In case of a transient wave packet, the linear term governs the propagation. Close to the wave board, we register a long and low wave train. Due to the small steepness a linear description is justified, i. e. the surface elevation can be expressed by

$$\zeta_1(t_i, x_l) = \frac{1}{2\pi} \sum_j F(\omega_j, x_l) e^{i\omega_j t_i} \triangle\omega \qquad (26)$$

in discrete form, with F as Fourier transform of the linear wave train. The amplitude of the harmonic wave is substituted by the envelope $a(t_i)$ of a linear wave packet as in case of a regular wave the amplitude is equivalent to the envelope ($a_k(t) = \zeta_a$). The wave packet envelope is calculated by Hilbert transform:

$$a(t_i) = \sqrt{\zeta_1^2(t_i) + \left(\sum_j F(\omega_j, x_l) \cdot e^{i(\omega_j t_i - \frac{\pi}{2})}\right)\triangle\omega)^2}. \qquad (27)$$

Following the Stokes-III analogy, the surface profile is expressed by

$$\begin{aligned} \zeta(t_i) &= \frac{\triangle\omega}{2\pi} \cdot \sum_j [|F(\omega_j, x_l)| e^{i(\omega_j t_i + \varphi)} \qquad (28) \\ &+ \frac{a(t_i)k(\omega_j)}{2} |F(\omega_j, x_l)| e^{2i(\omega_j t_i + \varphi)} \\ &+ \frac{3}{8} a^2(t_i) k(\omega_j) \cdot |F(\omega_j, x_l)| e^{3i(\omega_j t_i + \varphi)}] \end{aligned}$$

with φ as phase spectrum of the linear wave train.

Fig. 7 confirms the high accuracy using these tools for non-linear calculation of the moving frame wave train: The wave train (transient wave packet) is measured at a stationary wave probe close to the position of the wave maker (x = 8.74 m) as well as at a down–stream position of the wave tank (x = 85.03 m). Finally, the lower diagram presents the wave train as registered on board of the towing carriage (mean velocity 1.65 m/s). Transformation of the first wave train to the fixed down-stream position as well as to the moving wave probe travelling with the carriage is also shown. Agreement of registration and calculation (dots) is satisfactory.

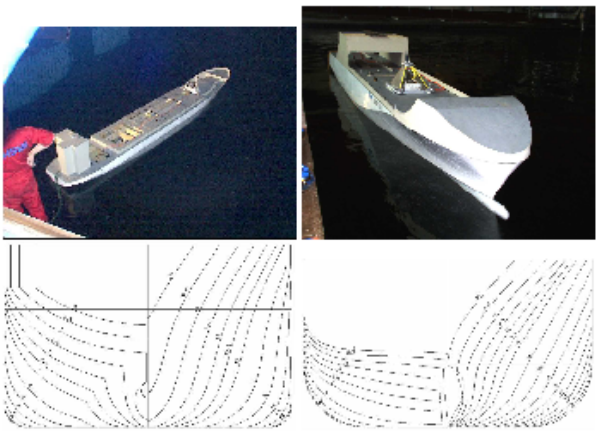

Figure 8: Investigated ship models and corresponding ship lines (left: C-Box – model scale 1:29 – right: RO-RO vessel – model scale 1:34).

4. RESULTS

In the framework of the ROLL-S project 100 analyzable capsizing test runs have been realized varying the following test parameters:

- metacentric height
- model velocity
- target course
- type of model sea
- characteristic wave period and height

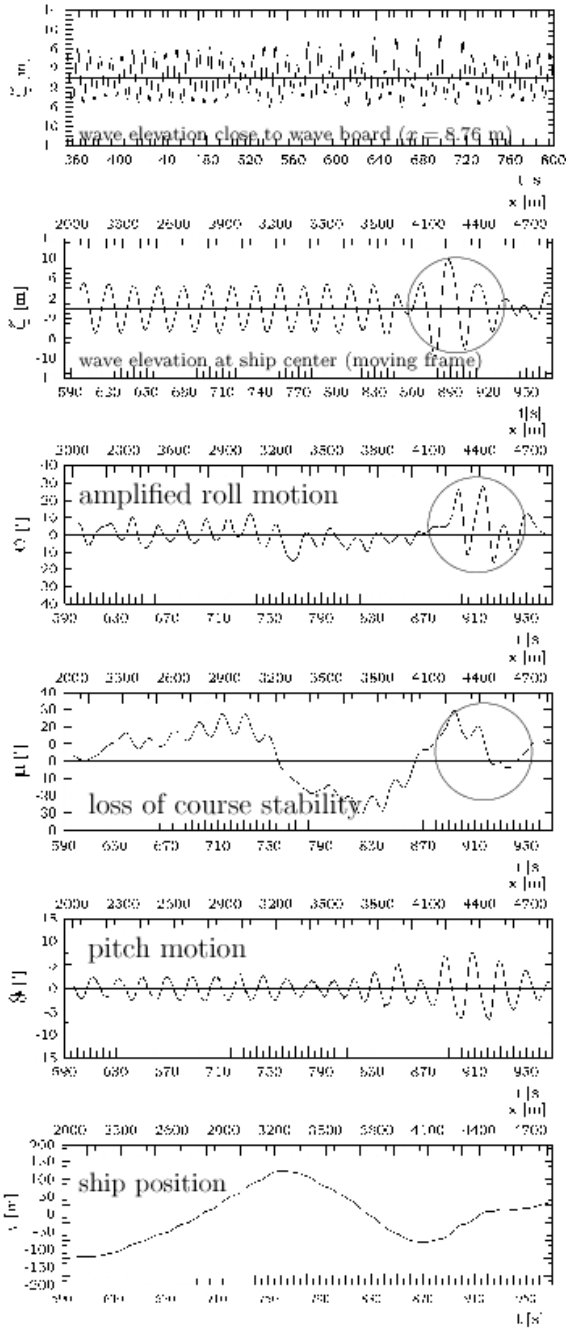

Figure 9: Roll motion of the C-Box (GM = 0.44 m, υ = 14.8 kn und μ = ± 20º) in a regular wave from astern (λ= 159.5 m, ζ_{crest} = 5.8 m) with proceeding high transient wave packet.

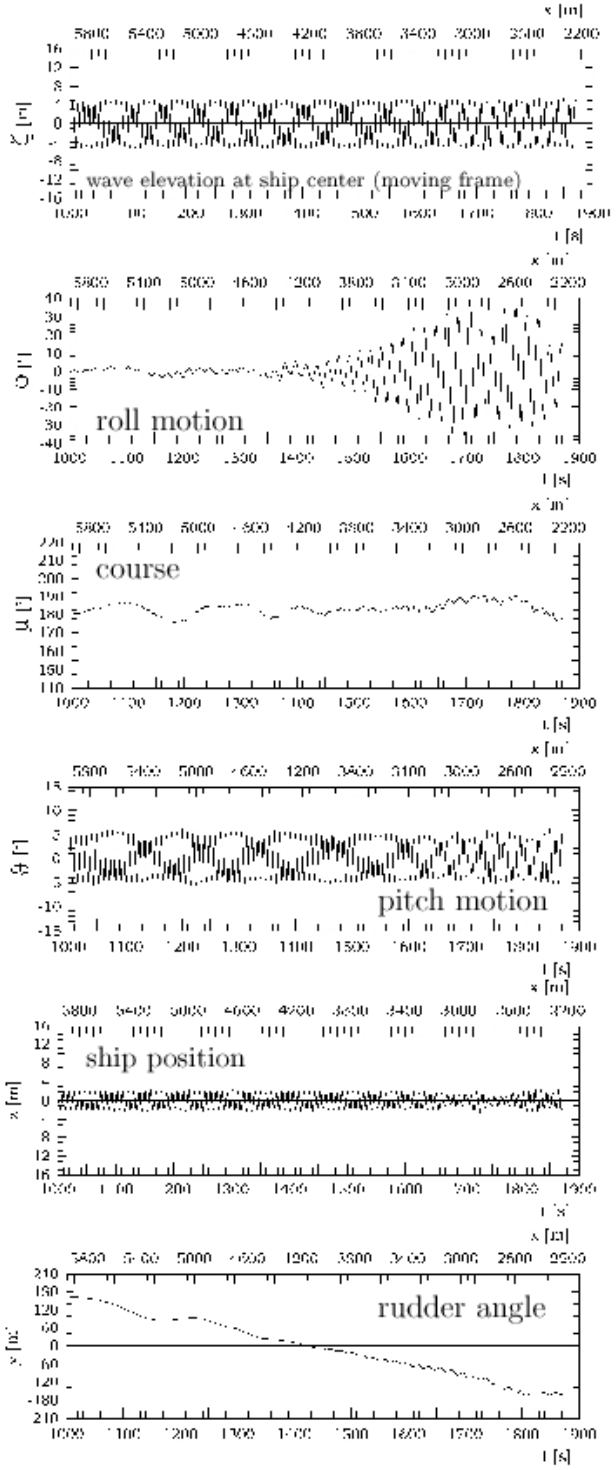

Figure 10: Parametric excitation of the RO-RO vessel at GM = 1.36 m, υ = 8 kn, at regular head seas, λ/L_{pp} = 1.2 m and H = 10.2 m.

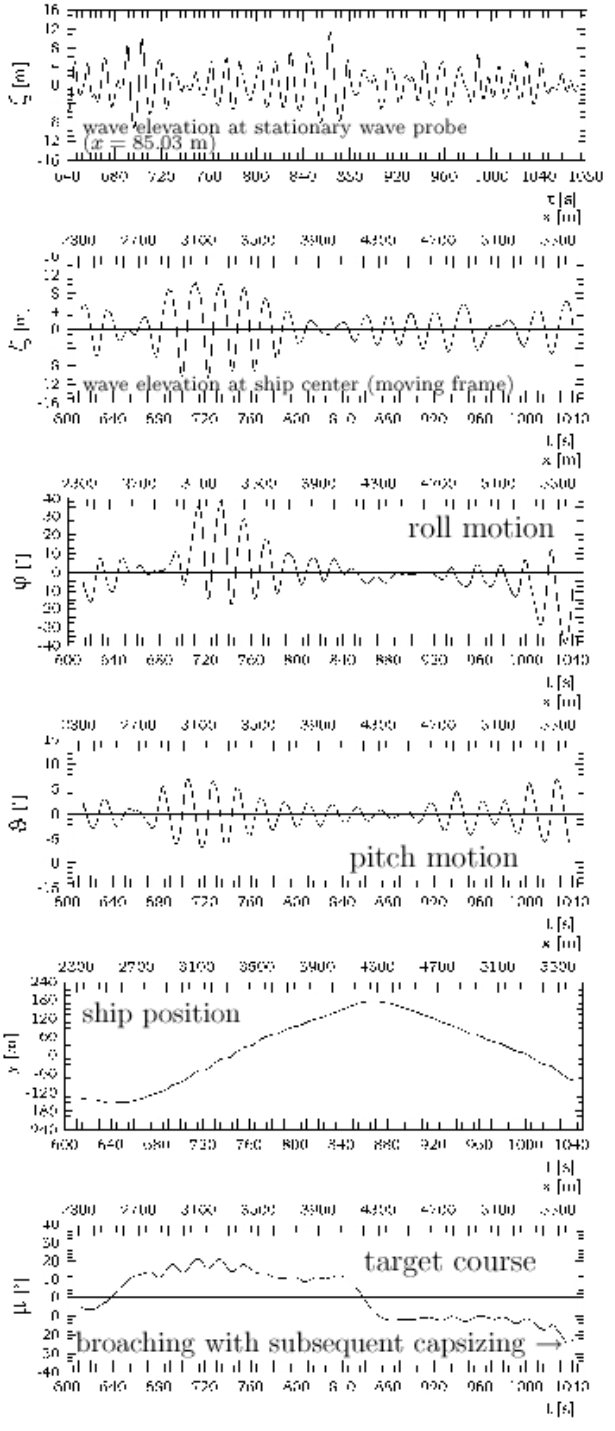

Figure 11: Broaching of the RO-RO vessel (GM=1.36 m, υ = 15 kn, Z-manoeuvre at μ = ± 10º) with subsequent capsizing in harsh seas (Tp = 14.6 s, Hs = 15.3 m).

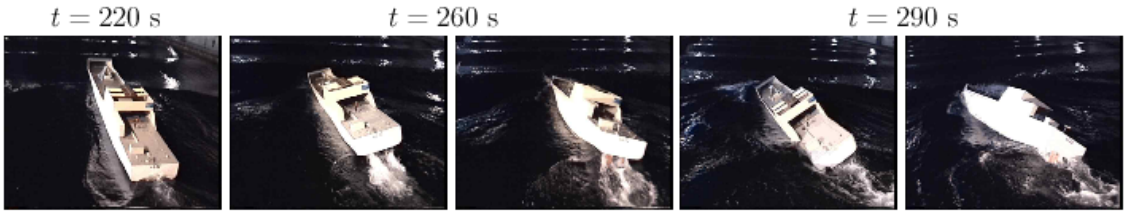

Figure 12: Parametric excitation of the RO-RO vessel (compare Fig. 10) — model scale 1:34.

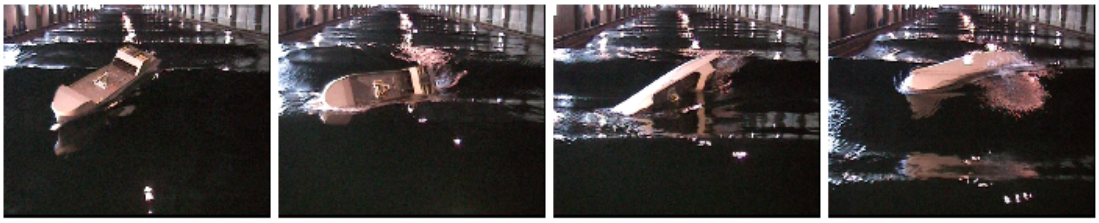

Figure 13: RO-RO vessel in a severe model storm (compare Fig. 11) – model scale 1:34.

Two ships – built by Flensburg Shipyard – have been investigated here:

• a multipurpose container vessel (C-Box) with L_{pp} =145.75 m, B =23.60 m, T = 9.00 m, and C_B = 0.7395 (model scale 1:29), and
• a RO-RO vessel with L_{pp} =182.39 m, B =26.00 m, T =5.70 m, and C_B = 0.5686 (model scale 1:34).

The models are self-propelled - the C-Box with one, the RO-RO vessel with two propulsion systems, which are controlled via telemetry by the master computer at the towing carriage (Fig. 8).

The application of the proposed experimental procedure is demonstrated in the following model tests. Fig. 9 shows test results for the C-Box measured in a regular wave from astern followed by a high transient wave packet. Note that a highly sophisticated wave generation technique is required to obtain such an apparently simple wave train at ship centre (moving frame) (see wave registration close to main board). Ship motions at all degrees of freedom have been registered optically - position, roll, pitch, course, and rudder angle are given here. This test case illustrates the advantage of using tailored wave sequences: the ship behaves inconspicuously until it encounters the high transient wave. Thus, the ship behaviour can be clearly related to the wave sequence.

Fig. 10 and 12 illustrate the ship motion characteristics (GM=1.36 m, natural roll period T_R = 19.2s, υ =8 kn) in high regular head seas (H = 10.2 m, λ = 218 m, T = 11.8 s), with a target course angle of μ = 177º. During the first half of the test duration roll motion is inconspicuous (see photos in Fig. 12 at model time t = 220 s). Suddenly, beginning at model time t = 240 s parametric rolling with twice the wave encounter period is starting, with increasing roll angles up to critical values of 40 degrees (see Fig. 12: photos at model time t = 260 s and t = 290 s). Note that the pitch motions remain rather mode-rate.

Fig. 11 and 13 present model test results of a RO-RO vessel (GM=1.36 m, natural roll period T_R=19.2 s, υ=15 kn) in extremely high seas from astern (ITTC spectrum with Hs=15.3 m, T_P =14.6 s, Z-manoeuvre: target course μ = ± 10º).

The upper diagram presents the registration at a stationary wave probe. As the waves are quite high the associated crests are short and steep followed by at and long troughs. In contrast, the cruising ship – see wave elevation at ship centre (moving frame)– apparently experiences extremely long crests and short troughs with periods well above 20 s as the vessel is surfing on top of the waves.

Consequently, the ship broaches, and finally capsizes as the vessel roll exceeds 40º and the course becomes uncontrollable (Fig. 13).

Note that the wave elevation refers to the moving frame at the centre position of the cruising ship, and can be directly correlated to the ship motions by magnitude and phase. As a consequence, the sea-keeping behaviour and even the mechanism of capsizing can be deduced and explained on the basis of non-linear cause-effect chains.

A large variety of model tests simulating different dangerous scenarios have been performed for the validation of numerical models, which are directly used to improve ship design and operation.

For bench-marking, the non-linear numerical methods are validated by dedicated sea-keeping model tests in deterministic wave sequences. By systematic simulations the most critical conditions are identified [4], [5]. As an example, Fig. 14 shows polar plots for two different load cases which illustrate at which course and speed the RO-RO ship is cruising safely (limiting roll angle 35º).

Based on these developments methodologies for the quantitative assessment of capsizing risk are proposed which then provide a basis for the improvement of current intact stability criteria. In conclusion ships are designed with improved sea-keeping characteristics and an increased safety with respect to the danger of extreme roll angles and capsizing. As a consequence, evaluation methods for capsizing risks are developed, and stability criteria improved.

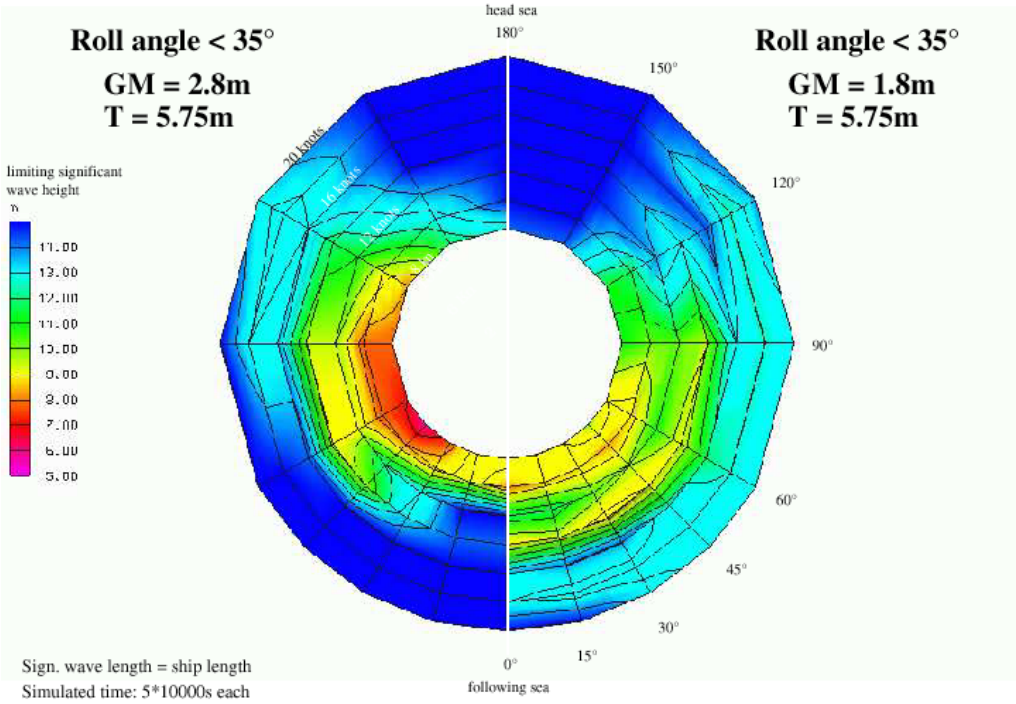

Figure 14: Polar plot with limiting wave heights for a RO-RO design - based on non-linear calculation methods.

5. CONCLUSIONS

The proposed accurate computer controlled sea-keeping test procedure is based on linear wave theory which is expanded by empirical procedures to consider the higher phase velocity of steep waves as well as their asymmetry. The backbone of the new model testing technique is the generation of deterministic wave trains with embedded extremely high waves or wave groups which interact with the cruising ship at selected positions in the wave tank. From registrations and numerical calculations the wave field is known in space and time. In particular, the wave elevation at the ship centre, as related to the cruising vessel (encountering periods – moving frame) is deduced. As the associated ship motions are registered simultaneously, cause-effect relations can be evaluated, revealing the mechanism of the genesis of large roll motions (incl. parametric rolling) and capsizing. As a consequence, the sea-keeping behaviour and even the mechanism of capsizing can be evaluated on the basis of non-linear cause and effect chains since the methods for generating and analyzing tailored wave trains allow calculations of the measured wave train in terms of a moving reference frame of the ship. Based on systematic experimental tests of the type presented here a non-linear numerical method for simulating ship motions in extreme seas has been developed. With this program polar plots are determined presenting limiting wave heights for the capsizing of a vessel depending on its speed and course. The assessment of the sea-keeping behaviour of a floating structure requires a highly complex procedure combining non-linear numerical simulation methods validated by deterministic sea-keeping tests. As a result, safer ships can be designed and loading and cruising conditions optimized, improving ship operation and navigation significantly.

6. ACKNOWLEDGEMENT

The authors are indebted to the German Federal Ministry of Research and Education (BMBF) for funding the projects ”ROLL-S” and ”SinSee”. Within these frameworks the presented results have been achieved. After finalizing ROLL-S we highly appreciate the approval of the new project ”SinSee” which allows further applications of the achieved results to promote the development of sophisticated analysis tools like neural networks. We thank all our ROLL-S partners for the fruitful cooperation — special thanks to the Hamburg Ship Model Basin and the Flensburg Shipyard.

7. REFERENCES

[1] J. Bergmann. Gaußsche Wellenpakete — Ein Verfahren zur Analyse des Seegangsverhaltens meerestechnischer Konstruktionen. PhD thesis, Technische Universität Berlin (D 83), 1985.

[2] G.F. Clauss and W.L. Kühnlein. A new approach to sea-keeping tests of self-propelled models in oblique waves with transient wave packets. In OMAE 95 -350, Copenhagen, June 1995.

[3] G.F. Clauss, E. Lehmann, and C. Östergaard. Offshore Structures, volume 1: Conceptual Design and Hydrodynamics. Springer Verlag London, 1992.

[4] H. Cramer and S. Krüger. Numerical Capsizing Simulations and Consequences for Ship Design. In STG Summermeeting Gdansk, Poland, 2001.

[5] H. Cramer and J. Tellkamp. Towards safety as a performance criteria in ship design. In RINA, editor, Passenger Ship Safety, International Conference, London, 2003.

[6] G.D. Crapper. Introduction to Water Waves. Ellis Horwood Limited, 1984.

[7] M.C. Davis and E.E. Zarnick. Testing ship models in transient waves. In 5 th Symposium on Naval Hydrodynamics, 1964.

[8] D. Faulkner. Rogue waves – Defining their Characteristics for Marine Design. In Rogue Waves 2000, Brest, France, 2000.

[9] S. Haver. Some Evidences of the Existence of Socalled Freak Waves. In Rogue Waves 2000, Brest, France, 2000.

[10] S. Haver and O.J. Anderson. Freak Waves: Rare Realization of a Typical Population or Typical Realization of a Rare Population? In Proceedings of the Tenth International Offshore and Polar Engineering Conference, pages 123–130. ISOPE, Seattle, USA, 2000.

[11] P. Kjeldsen. A sudden disaster – in extreme waves. In Rogue Waves 2000, Brest, France, 2000.

[12] S.P. Kjeldsen. Determination of severe wave conditions for ocean systems in a 3-dimensional irregular seaway. In Contribution to the VIII Congress of the Pan-American Institute of Naval Engineering, pages 1–35, 1983.

[13] W. Kühnlein. Seegangsversuchstechnik mit transienter Systemanregung. Dissertation, Technische Universität Berlin (D 83), 1997.

[14] W.K. Kühnlein and K.E. Brink. Model Tests for the Validation of Extreme Roll Motion Predictions. In OMAE 2002 – Proceedings of 21st Conference on Off-shore Mechanics and Arctic Engineering, Oslo, Norway, 2002. OMAE2002-28269.

[15] W.L. Kühnlein, G.F. Clauss, and J. Hennig. Tailor made freak waves within irregular seas. In OMAE 2002 - 21st Conference on Offshore Mechanics and Arctic Engineering, Oslo, 2002. OMAE2002-28524.

[16] M. Schulz. ”Ich spürte den Atem Gottes”. Der Spiegel, December 2001. No. 51/2001.

[17] S. Takezawa and T. Hirayama. Advanced experimental techniques for testing ship models in transient water waves. Part II: The controlled transient water waves for using in ship motion tests. In R. Bishop, A. Parkinson, and W. Price, editors, Proceedings of the 11th Symposium on Naval Hydrodynamics: Unsteady Hydrodynamics of Marine Vehicles, pages 37–54, 1976.

[18] K. Trulsen and K. Dysthe. Freak Waves a three-dimensional wave simulation. In Proceedings of the 21st Symposium on Naval Hydrodynamics, pages 550–558, 1997.